Heat Shrinkable Polymer Blends Based on Grafted Low Density Polyethylene and Chlorosulfonated Polyethylene (Part-II)

J. K. Mishra[a]; S. Raychoudhury[a]; C. K. Das[a]

[a] Materials Science Centre, IIT, India

PLEASE SCROLL DOWN FOR ARTICLE

Heat Shrinkable Polymer Blends Based on Grafted Low Density Polyethylene and Chlorosulfonated Polyethylene (Part - II)

J. K. MISHRA, S. RAYCHOUDHURY and C. K. DAS*

Materials Science Centre, IIT, Kharagpur 721302, India

Heat shrinkability of the polymer which depends on elastic memory can be introduced into the system in the form of an elastomeric phase. The present study deals with the measurement of heat shrinkability of the blend of grafted polyethylene and CSM. Interchain crosslinking between grafted polyethylene and elastomer improved the shrinkability. Maleic anhydride and glycidyl acrylate is used as grafting materials. Glycin and 4 4′ diamino diphenyl sulphone is used as coupling agents. Maximum amount of crosslinking is obtained when glycidyl acrylate is used as grafting agent. Minimum amount of interchain crosslinking is observed when 4 4′ diamino diphenyl sulphone is used as coupling agent. Probable interactions of rubber and plastic phase are confirmed by IR spectroscopy. Extraction of the elastomeric phase is restricted due to interchain crosslinking as confirmed by SEM study which is more prominent in the case of glycidyl acrylate grafted LDPE.

Keywords: Low density polyethylene; chlorosulfonated polyethylene; shrinkability; grafting

INTRODUCTION

Blending appears to be a powerful technique for polymer modification. By means of blending different polymers with several properties can be improved while retaining other properties [1 – 2]. It is now clear

---

*Corresponding author.

that nearly all blends are comprised of one polymer domain dispersed in the matrices of other polymer [3 – 4]. Thermoplastic elastomers have gained considerable attention, in recent years from shrinkability point of view [5 – 7]. Recently Das et al. [8] have studied the heat shrinkable behaviour of Polyolefine blends with elastomer like CSM. They suggested the importance of a crosslinked elastomeric phase to enhance the heat shrinkability of a blend system and at the same time to improve their flame retardency. Here, the aim is to study the effect of the interchain crosslinking on shrinkability of the blends comprised of elastomer and plastic. LDPE was grafted initially to prepare the interchain crosslinked blend with hypalon.

EXPERIMENTAL

The blending formulations were shown in Table I. The used LDPE was 22 FA with MFI 0.20 and density 0.912 gm/cc, from IPCL, India. The CSM was Hypalon – 40 grade of Du-Pont, USA. The blend ratio of LDPE/CSM was taken as 60 : 40 which were melt blended in a brabender plasticorder for 10 minutes at 20 rpm. The temperature of mixing was 120°C. In presence of coupling agents and grafting materials the blends were cured in a compression mold for half an hour at 150°C at 4T pressure. The vulcanizates were stretched both at ambient and elevated temperatures. The room temperature stretched samples were allowed to shrink at 150°C. The other samples were allowed to shrink at that temperature in which they were stretched. The lengthwise shrinkage was measured at various temperatures according to the formula,

$$\text{Sh}\% = \frac{L_{Str} - L_{Shr}}{L_{Str}} \times 100$$

TABLE I   Mixing formulations

Sample	LDPE (phr)	DCP (phr)	Hypalon (phr)	Maleic anhydride (phr)	Glycin (phr)	4 4' diamino diphenyl sulphone (phr)	Glycidyl acrylate (phr)
1	60	0.2	40	4	2	–	–
2	60	0.2	40	4	–	2	–
3	60	0.2	40	–	–	–	4

Where, Sh% = percentage shrinkage

L_{Str} = Length of the sample after stretching

L_{Shr} = Length of the sample after it was shrunk

The cure characteristics were studied using a Monsanto Rheometer (R-100) at 150°C temperature. The X-ray diffraction were studied using PW-1840 X-ray diffractometer with Cobalt target (Cokα). The chart speed was 10 mm/2θ, slit of 0.2 mm applying 40 KV, 20 mA current in order to have the idea of crystallinity of the blends as affected by the extent of stretching. The area under the crystalline and amorphous portion was determined in arbitary units: the degree of crystallinity χ_c and the amorphous content (χ_a) were measured, using the relationship:

$$\chi_c = I_c/(I_a + I_c); \quad \chi_a = I_a/(I_a + I_c)$$

where I_c and I_a are the integrated intensities corresponding to crystalline and amorphous halo respectively.

Peak half width (β), crystallite size (P), interchain distance (r) and interplanar distance (d) were calculated as follows [9].

$$\beta = \text{Area of peaks}/\text{Height of peak} \times 1/5$$

$$P = 92.35/\beta \cos \theta$$

$$r = 5/8 \times \lambda/\sin \theta$$

$$d = 1.79/2 \sin \theta \ (\lambda = 1.79 \ \overset{\circ}{A})$$

DSC/TGA studies were carried out using Stanton Redcroft STA-625 thermal analyser, in the temperature range 25°C to 600°C at a heating rate of 10°C/min in air to get the idea of degradation pattern. Phase morfology was studied using specimens after differential solvent extraction with the help of a scanning electron microscope, SEM (Cam Scan series 2 and E 5200 auto sputter coater).

RESULTS AND DISCUSSION

Effect of Temperature on Shrinkability

The percentage shrinkability at various temperatures is shown in Table II. It was observed that for all the samples the shrinkability was always less for room temperature stretched sample. Shrinkability at 150°C was always maximum compared to 120°C or 180°C. This is

TABLE II   Heat shrinkability of the blends at different temperatures

Sample	Room temp.	120°C	150°C	180°C	210°C
1	70	75	83	78.6	–
2	75	84.4	87	80	–
3	71	78	84.6	82.1	80

probably due to the moderate viscous flow at 150°C, which helps the stretching. The sample-3 gives excellent Shrinkability even at 210°C. But at 120°C the plastic phase is in partially molten state and at 210°C the same flows vigorously which again may oppose the stretching. Again, uniform stretching at 150°C does not develop any unfavourable condition in shrinkage. In the case of sample-3 the amount of crosslinking is high that consequently gives the shrinkage even at 210°C unlike others.

Effect of Crosslinking on Shrinkability

Continuous cure characteristic is observed through Monsanto Rheometer, R-100 and it is shown in Figure 1. Torque is found to increase in sample-3, but is not increasing in other samples. So, the observed interchain crosslinking was maximum in the sample 3. Though very less amount of crosslinking occurs in case of sample-1 and sample-2, but this is not reflected due to the presence of plastic phase which is already in molten state at 150°C temperature. But in case of sample-3 as the amount of crosslinking is substantial, and exceeds the effect of molten plastic state and is reflected in torque rheomatry. This trend is also confirmed by swelling coefficient study and is shown in Table V.

Effect of Crystallinity on Shrinkability

X-ray diffraction diagram of various blends are shown in Figures 2, 3, 4. The change of parameters associated with X-ray diffraction are produced in Table III. It is seen that the crystallinity of R-T stretched sample is lower than the original sample (sample-3). But the crystallinity is continuing to increase at 150°C temperature and 210°C temperature on stretching. But the crystallinity of the shrunk sample (150°C) is very closed to the usual sample. At room temperature, due to stretching some crystal network may break down due to imposition of external longitudinal force. That is why crystallinity decreases, but at 150°C the
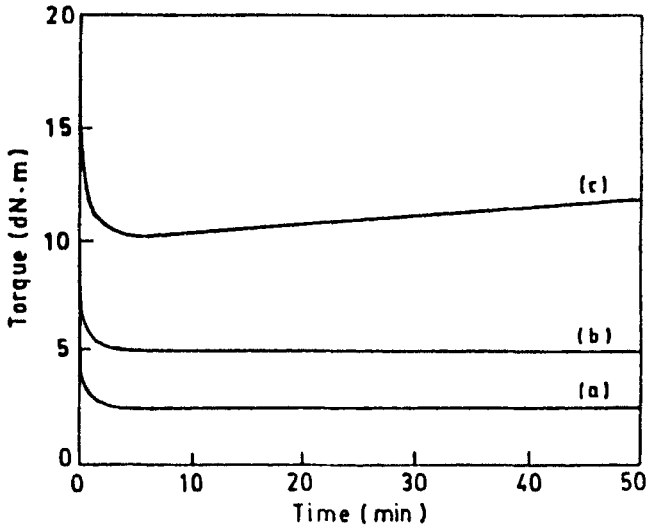
FIGURE 1   Rheometric plot of the blends at 150°C.
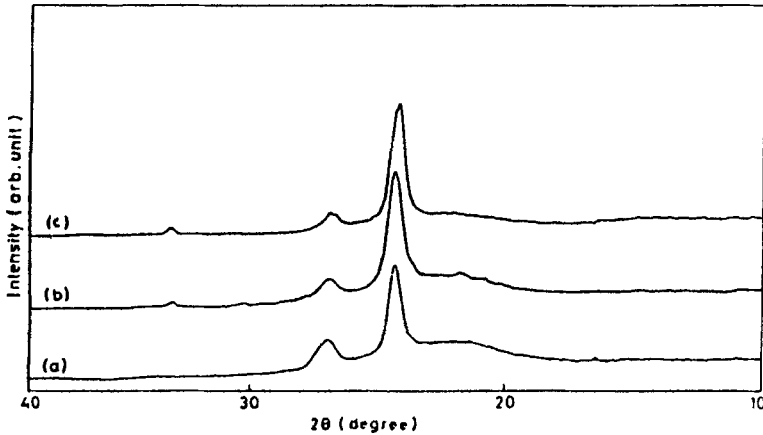
FIGURE 2   XRD of the Blend LDPE/DCP/Hypalon/Maleic anhydride/glycin (a) Usual sample; (b) Stretched sample at 150°C; (c) Shrunk sample.

plastic phase is in molten state, so the mobility of the polymer chain is increased, as a result the nucleation and crystal growth is favoured, hence the crystallinity is increased at 150°C. At 210°C the mobility of the chain is again higher producing the greater crystallinity than that at
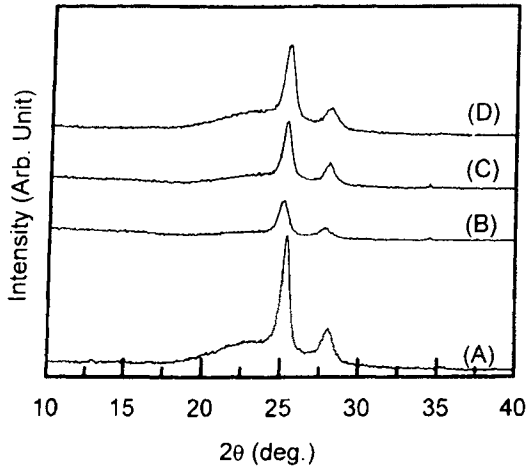
FIGURE 3   XRD of the Blend LDPE/DCP/Hypalon/Maleic anhydride/diamino diphenyl sulphone (A) Usual sample; (B) Stretched sample at 120°C; (C) Stretched sample at 150°C; (D) Shrunk sample.

FIGURE 4   XRD of the Blend LDPE/DCP/Hypalon/Glycidyl acrylate (A) Usual sample; (B) Room temperature stretched sample; (C) Stretched sample at 150°C; (D) Stretched sample at 210°C; (E) Shrunk sample.

150°C. During shrinkage the crystallinity is somewhat decreased due to loss of orientation as a result of recoiling. The trend is same in case of sample-1 and sample-2. The interchain distance and the inter planner

TABLE III X-ray diffraction parameters

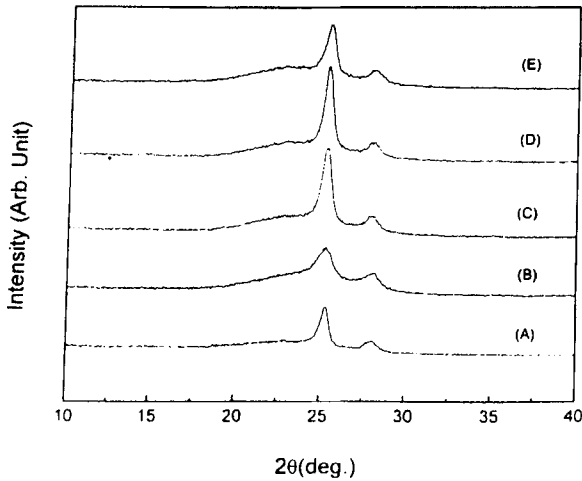| Sample code | Peak angle | | Percent crystal-linity | Percent amorphity | Inter-planner distance ($\overset{\circ}{A}$) | Crystal-lite size ($\overset{\circ}{A}$) | Interchain distance ($\overset{\circ}{A}$) |
	Low	High					
Sample No. 1							
A-usual	12.55	14.0	30.3	69.7	4.12	157.7	5.73
B-stretched (150°C)	12.65	13.9	24.79	75.21	4.09	147.8	5.69
C-shrunk (150°C)	12.35	13.7	28.0	72.0	4.19	152.2	5.82
Sample No. 2							
A-usual	12.64	14.01	36.4	63.6	4.09	182.68	5.40
B-stretched (120°C)	12.52	13.87	39.01	60.99	4.12	182.61	5.38
C-stretched (150°C)	12.60	13.98	41.14	58.86	4.10	177.29	5.32
D-shrunk (150°C)	12.64	14.00	38.2	61.8	4.09	179.80	5.41
Sample No. 3							
A-usual	12.63	14.01	33.1	66.90	4.09	177.30	5.48
B-stretched (R.T)	12.60	14.00	24.1	75.90	4.10	164.47	5.34
C-stretched (150°C)	12.61	13.98	34.37	65.63	4.09	167.74	5.41
D-stretched (210°C)	12.63	13.98	37.76	62.24	4.09	181.54	5.41
E-shrunk (150°C)	12.65	14.01	32.05	67.95	4.08	168.60	5.49

distance remains almost unchanged for all the samples. But when the focus is pointed to the crystallite size, some appreciable change is observed. With stretching the crystallite size is decreased. The crystallite of room temperature stretched sample is lower than the stretched sample at 150°C which again is less than the shrunk sample. It is found that, shrinkability increases as crystallite size increases though the flow behaviour has a great role in shrinkability.

Thermal Analysis

The TGA/DSC plots are shown in Figure 5 and the parameters obtained are given in Tables IV and V. It is obvious from the table that the degradation goes through two steps and the trend of change in first
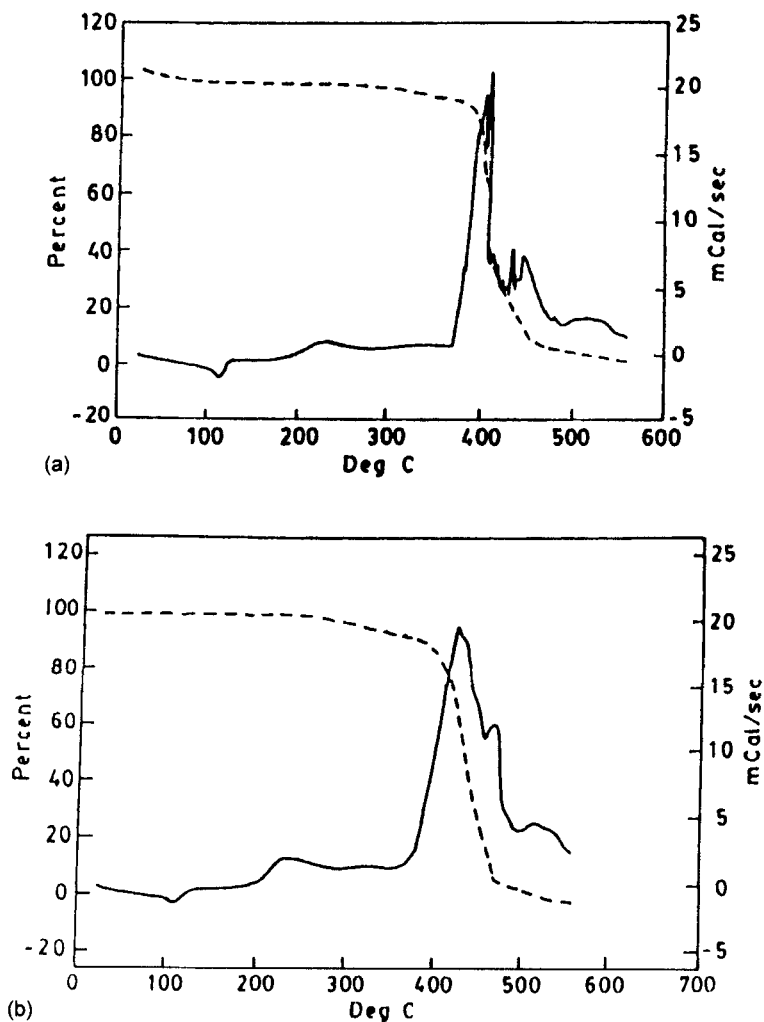
FIGURE 5   TGA/DSC plot of the blends (a) LDPE/DCP/Hypalon/Maleic anhydride/
diaminodiphenyl sulphone; (b) LDPE/DCP/Hypalon/Glycidyl acrylate.

TABLE IV   DSC/TGA Results

Sample	First degradation temp. (°C)	Second degradation temp. (°C)	Heat of degradation(mCal/mg)	
			H_1	H_2
1	276	358	24	262
2	284	369	28	288
3	292	383	54	321

TABLE V   DSC/TGA Results

Sample	Onset temp. of crosslinking (°C)	Heat of crosslinking (mCal/mg)	Swelling coefficient
1	201	38.2	0.96
2	192	49.6	0.93
3	188	62.0	0.58

as well as the second degradation temperature are same, the lowest for sample-1 and highest for sample-3 and the sample-2 is having the value in between. So, it can be concluded that, the sample-3 is most stable during both the steps and the sample-1 is least stable. This may be due to the highest amount of interchain crosslinking occurred in case of sample-3 and lowest amount in sample-1. This is also supported by torque rheometry.

Again the heat of degradation associated with first degradation and second degradation are viewed to be in the same line, highest is for sample-3 and lowest for sample-1. Larger amount of heat of degradation means larger amount of degradation, assuming the reaction to be an exothermic. So from the thermal parameters it can be concluded that the degradation starts at higher temperature in case of sample-3, but the degradation is rapid in this case for the both the steps. Again for sample-1, degradation starts earlier, but the process is slower compared to sample-2 and sample-3 for both steps of degradation.

Again, from the onset temperature of crosslinking and the heat of crosslinking of the samples, it is obvious that for sample-3, the onset temperature of crosslinking is lowest but the heat of crosslinking is highest, so crosslinking is started earlier and the reaction of crosslinking is rapid and the extent of crosslinking is also highest in this case. On the other hand, for sample-1, reaction started at higher temperature and the amount of heat of crosslinking is lower. For sample-3, the extent of crosslinking is highest, and showed highest amount of shrinkability. For the similar reason, for sample-1 the shrinkability is lowest with lowest interchain crosslinking.

IR Spectrum of the Blends

Sample-1

Figure 6a represents the IR spectrum of the sample-1. Chlorosulphonated polyethylene shows two absorption bands at $1160\,cm^{-1}$ and
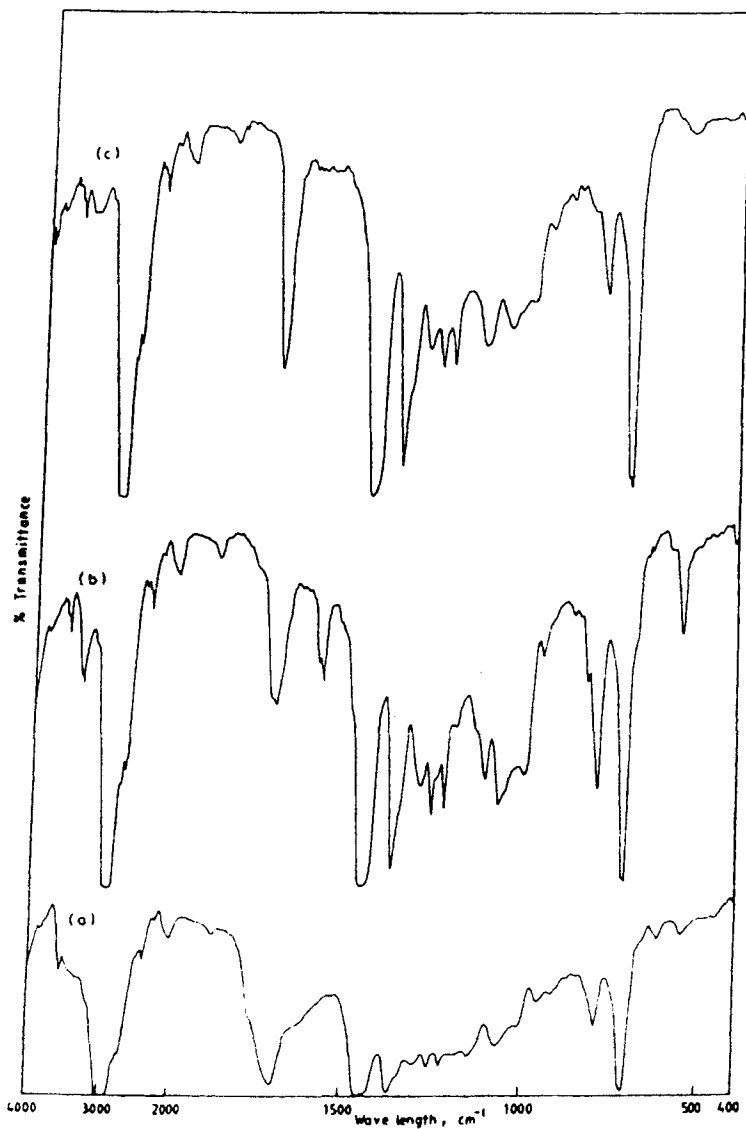
FIGURE 6   IR Spectra of the Blend (a) Sample no. 1; (b) Sample no. 2; (c) Sample no. 3.

$1368 \, cm^{-1}$ which are assigned to symmetric and asymmetric stretching of SO_2 group in CSM [10]. From IR it is observed that, one band appeared at $1649 \, cm^{-1}$ which corresponds to the stretching of the

carbonyl group of imide ring. Carbonyl group of anhydride which appears at $1760\,cm^{-1}$ and $1810\,cm^{-1}$ are absent in the IR of the blend. Step-I is already reported [11]. The absence of anhydride carbonyl group and the presence of the imide carbonyl group confirms the reaction of the Step-II. Again in the blend symmetric stretching frequency of SO_2 group appears at $1139\,cm^{-1}$. This is due to the change of environment of the SO_2 group from chlorine to oxygen, directly attached to SO_2 [12]. This change confirms the reaction of Step-III. Much emphasis is not given to the asymmetric stretching frequency of SO_2 ($1368\,cm^{-1}$) as this may overlap with the CH_3 deformed mode at $1378\,cm^{-1}$ and CH_2 wagging mode at $1368\,cm^{-1}$[13].

Sample-2

Figure 6b represents the IR spectrum of the sample-2. From the IR it is observed that, one band appeared at $1712\,cm^{-1}$ which corresponds to the stretching of carbonyl group in the imide ring. Carbonyl group of the anhydride which should have been appeared at $1760\,cm^{-1}$ and $1810\,cm^{-1}$ are absent in the IR of the blend. Step-I is already reported. The absence of anhydride carbonyl group and the presence of imide carbonyl group confirms the reaction of the Step-II. Chlorosulpho-

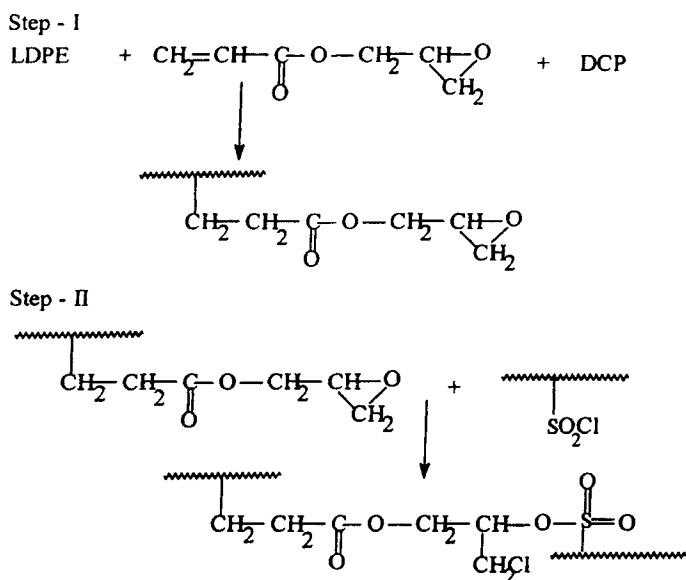nated polyethylene shows two absorption bands at $1160\,cm^{-1}$ and $1368\,cm^{-1}$ which are assigned to symmetric and asymmetric stretching frequency of SO_2 group. Again, one strong band is observed at $1155\,cm^{-1}$, so there is a shift of SO_2 stretching (symmetric) frequency towards lower side. So, from this observation, Step-II has been confirmed. Again in this case also much emphasis is not given to the symmetric stretching frequency of $SO_2(1368\,cm^{-1})$. Because the CH_3 deformation mode at $1378\,cm^{-1}$ and CH_2 wagging mode 1368 and $1355\,cm^{-1}$ contribute to the band absorbtion.
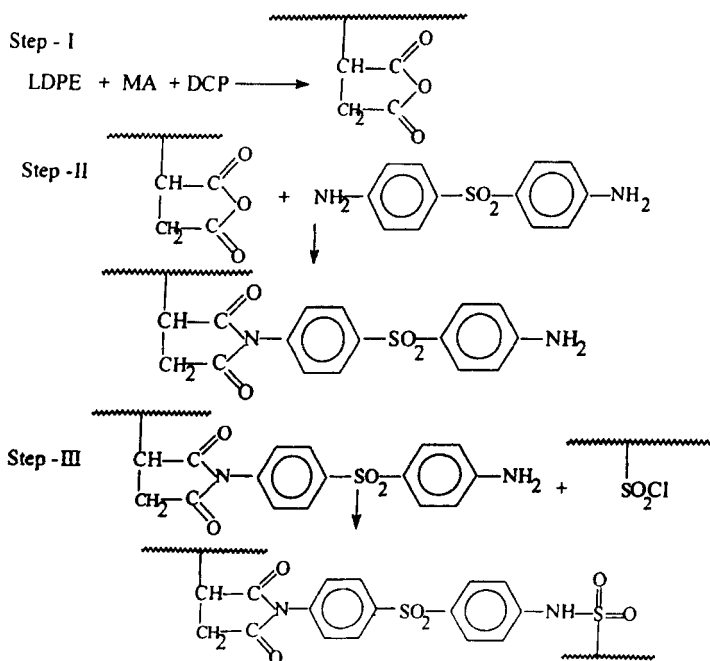
Sample-3

Figure 6c represents the IR spectrum of the sample-3. The spectra reveals that there is no band at 1000, 900, $850\,cm^{-1}$ which are the characteristics of epoxy group. Hence it can be said that epoxy group of the grafted polyethylene involves in the crosslinking reaction.

Original chlorosulphonated polyethylene has two strong absorbtion bands at $1160\,cm^{-1}$ and $1368\,cm^{-1}$. They are due to the symmetric and asymmetric stretching modes of SO_2 respectively. In the blend symmetric stretching frequency appears at $1133\,cm^{-1}$. The shift is due to the change of environment of SO_2 group from chlorine to oxygen directly attached to sulpher. This change in enviroment is due to the involvement of the $-SO_2Cl$ group in the interchain crosslinking reaction. From the above discussion the probable mechanism may be as below. The Step-I is already reported [14].

Step - I

$$\text{LDPE} \quad + \quad CH_2=CH-\overset{\displaystyle O}{\underset{\displaystyle}{C}}-O-CH_2-CH-\overset{O}{\underset{CH_2}{\diagup}} \quad + \quad \text{DCP}$$

$$\downarrow$$

$$\sim\!\!\!\sim\!\!\!\sim CH_2-CH_2-\overset{\displaystyle O}{\underset{\displaystyle}{C}}-O-CH_2-CH-\overset{O}{\underset{CH_2}{\diagup}}$$

Step - II

$$\sim\!\!\!\sim\!\!\!\sim CH_2-CH_2-\overset{\displaystyle O}{\underset{\displaystyle}{C}}-O-CH_2-CH-\overset{O}{\underset{CH_2}{\diagup}} \quad + \quad \sim\!\!\!\sim\!\!\!\sim SO_2Cl$$

$$\downarrow$$

$$\sim\!\!\!\sim\!\!\!\sim CH_2-CH_2-\overset{\displaystyle O}{\underset{\displaystyle}{C}}-O-CH_2-CH-O-\overset{\displaystyle O}{\underset{\displaystyle O}{S}}=\;\;\sim\!\!\!\sim\!\!\!\sim$$
$$\underset{\displaystyle CH_2Cl}{}$$

SEM Study

The phase morphology of the blends (High temperature shrunk sample) have been studied by scanning electron microscope. After the solvent extraction by toluene to remove the CSM phase for the blends 1 and 3 and represented in the Figures 7a and 7b. It is evident from the Figure 7a that the CSM phase is easily removed from the system where as the Figure 7b showed that the removal of CSM phase is being restricted. This study clearly revealed that the easy extraction is due to
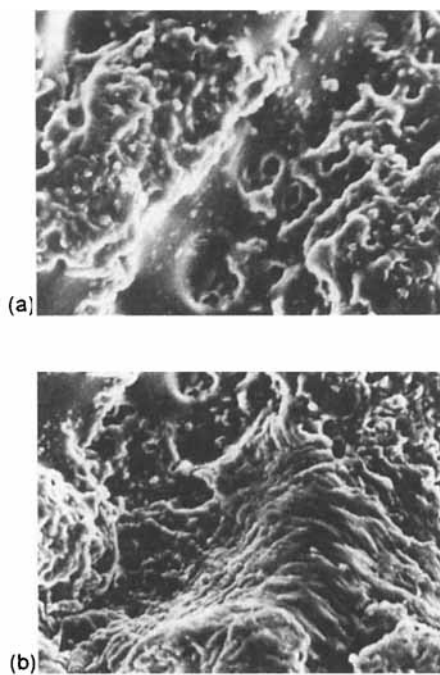
FIGURE 7   SEM photograph of the blend (a) Sample no. 1 (×1000); (b) Sample no. 3 (×1000).

the lack of interphase adhesion which is more in the case when glycin is used as a coupling agent. Glycidyl acrylate seems to be a efficient interchain crosslinker between the LDPE and CSM.

CONCLUSION

Heat shrinkability of H-T stretched sample is higher than that of R-T stretched one. Moderate flow of plastic phase favours the heat shrinkability, so the heat shrinkability at 150°C is highest. Shrinkability increases as the interchain crosslinking increases. Increasing crystallite size enhances the shrinkability, though the flow behaviour has a great role in shrinkability as effected by the presence of elastomeric phase. Moreover, it is noticed that the higher the amount of degradation (as in sample-3) the higher is the amount of crosslinking and consequently higher will be the amount of shrinkability.

References

[1] Hess, W. M., *et al.* (1993). *Rub. Chem. Tech.*, **66**, 329.
[2] Coran, A. Y. and Lee, S. (1992). *Rub. Chem. Tech.*, **65**, 231.
[3] Mukhopadhya, P. and Das, C. K. (1990). *J. Appl. Polym. Sci.*, **39**, 49.
[4] Danesi, S. and Porter, R. S. (1978). *Polymer*, **19**, 448.
[5] Patra, P. K. and Das, C. K. (1997). *J. Reinforced Plastics and Composites*, **16**, 111.
[6] Patra, P. K. and Das, C. K. (1997). *Journal of Polymer Engineering*, **17**, 231.
[7] Patra, P. K. and Das, C. K. (1998). *Journal of Applied Polymer Science*, **68**, 597.
[8] Patra, P. K. and Das, C. K. (1997). *Intern. J. Polym. Mat.*, **35**, 103.
[9] Alexander, L. E., X-ray Diffraction in Polymer Science, Wiley Interscience, New York (1969).
[10] Benzamin Bikson, Joseph Jagur-Grodzinski and David Vofsi (1981). *Polymer*, **22**, 640.
[11] Gaylord, N. G. Mehta (1982). *J. Polym Sci., Polym. Lett.*, **20**, 481.
[12] Pavia Donald, L., Lampan Gary, M. and Kriz Georges, S. (1996). Introduction to Spectroscopy Harcourt Brace College Publisher.
[13] Roychowdhury, A. and Dey, P. P. (1993). *Rubber Chemistry and Technology*, **66**, 233.
[14] Gallucci robert, R. and Going Rose, C. (1982). *Journal of Applied Polymer Science*, **27**, 425.